Available online at www.sciencedirect.com
ScienceDirect
Cement and Concrete Research 36 (2006) 1894–1902
Cement and Concrete Research

Study of rehabilitation mortars: Construction of a knowledge correlation matrix

S.F. Marques [a], R.A. Ribeiro [b], L.M. Silva [b], V.M. Ferreira [c], J.A. Labrincha [a,*]

[a] *Ceramics and Glass Engineering Dept., CICECO, University of Aveiro, 3810-193, Aveiro, Portugal*
[b] *Saint-Gobain Weber Cimenfix, Aveiro, Portugal*
[c] *Civil Engineering Dept., CICECO, University of Aveiro, 3810-193, Aveiro, Portugal*

Received 11 May 2005; accepted 19 June 2006

Abstract

In old building rehabilitation practices, the gathering of full knowledge on used mortars is the most difficult task due to their complexity and variability. At the same time, this necessity of knowledge is critical, since the rehabilitation work must guarantee physical, chemical and mechanical compatibility between former and restoration mortars, not relinquishing aesthetic details. However, the characterization of old mortars can be a very complex process, since it involves different techniques and potentially controversial outcomes.

In this work, several mortars were prepared and characterized, in order to improve knowledge that will facilitate the further choice of a suitable material to replace any old mortar. Analytical techniques like XRD and DTA/TGA were used in the determinations of chemical compositions, and physical properties determinations (apparent density, open porosity, compression strength, flexural strength, elastic modulus) were important to understand the mechanical behaviour and durability and to relate it with the prepared formulations composition.

Keywords: Old mortars; Rehabilitation; Physical–chemical compatibility; Characterization

1. Introduction

The maintenance and restoration of old mortars is one of the key aspects of correct construction rehabilitation practice. The main concern is to preserve the aspect and the quality, if possible with the use of the original technology, in order to assure the continuity with the past. However, the gradual disappearance of some materials and of the practical working experience has brought some difficulties [1].

To assure correct restoration work it is necessary to guarantee the physical–chemical and mechanical compatibility between rehabilitation mortars and the old mortars, regarding the original aspect and taking into account that the reintegration must be reversible and easily recognised. Carrington and Swallow [2] emphasised the advantages of using weaker and higher porosity mortars compared to the structural substrate, so they will have a sacrificial function in case of localised deterioration.

Mortars are used for several applications, so their constituents may vary significantly even in the same building. As an example, the binder might be aerial lime, hydraulic lime, cement and gypsum, while siliceous or calcareous sands are used as aggregates. As expected, strong variations of physical and mechanical properties of mortars are observed [3–6], making the identification of their constituents a complex task. Moreover, the occurrence of degradation reactions (e.g. weathering processes) might alter some original properties, increasing the complexity. As a result, significantly different properties may be achieved by thousands of different materials combinations, confirming the difficulty in defining rules and methodologies for the preparation of suitable rehabilitation mortars. Since the rehabilitation market has grown in the recent years, the classification of old mortars in distinct groups, depending on their physical–chemical characteristics, has become more important. Therefore, the use of advanced characterization techniques was proposed for old mortars [3,7–9], and some studies have reported for specific buildings, areas or

* Corresponding author. Tel.: +351 234370354; fax: +351 234425300.
E-mail address: jal@cv.ua.pt (J.A. Labrincha).

0008-8846/$ - see front matter © 2006 Elsevier Ltd. All rights reserved.
doi:10.1016/j.cemconres.2006.06.005

historical times [10,11]. Results may be useful to understand the complex properties/composition relationships.

The aim of the current work is to research these relationships through the preparation of several known formulations, followed by a full characterization by normalised techniques [12,13] and comparison with old mortars of common buildings. The constitution of a knowledge matrix will facilitate the selection of the suitable new mortar in rehabilitation works. The characterization techniques were divided in two groups: (i) distinctive techniques, permitting the identification of the mortar type (XRD or DTA/TGA analyses); and (ii) comparative techniques (e.g., mechanical strength and porosity determinations).

2. Experimental

2.1. Materials

Several mortars were prepared and characterized, varying the type and proportion of binder and aggregates. The formulations attempted to replicate some representative sets of old mortars. Aerial lime, hydraulic lime, Portland cement, gypsum, pozzolan-type material (red bricks powder) and mixtures of them were used as binders.

As aggregates, quartz sand, coarse siliceous sand (here named "chorreio") and calcareous sand ("micromar") were tested. Table 1 shows some chemical and physical characteristics of the used raw materials. Table 2 lists all tested formulations, including some

Table 1
Chemical and physical characteristics of the raw materials used

Raw material	Type	Particles size (μm)	ρ_{appar} (g/cm^3)	Composition (XRD)	
				Crystalline phases	Traces
Aerial lime	Hydrated lime	<80	0.39	Portlandite, calcite	–
Hydraulic lime	NHL 5-Cimpor	<160	0.60	Calcite, portlandite, belite	Quartz
Cement	I-42.5-Cimpor	<160	0.93	Belite, calcite, calcium aluminum iron oxide	–
Gypsum	By-hydrated calcium sulphate	<160	0.78	Gypsum	Quartz
Red bricks powder	–	<160	–	Quartz, muscovite	Hematite
Sand	Siliceous sand	160<∅<630	1.41	Quartz	–
Chorreio	Coarse siliceous sand	315<∅<1250	1.45	Quartz, microcline	Albite
Micromar	Calcareous aggregate	<630	1.49	Calcite	–

Portlandite: $Ca(OH)_2$; Calcite: $CaCO_3$; Belite: Ca_2SiO_4; Quartz: SiO_2; Calcium aluminum iron oxide: $Ca_2Fe_{1.4}Al_{0.6}O_5$; Gypsum: $CaSO_4{:}2H_2O$; Muscovite: $HAl_2(AlSi_3O_{10})(OH)_2$; Hematite: Fe_2O_3; Microcline: $KAlSi_3O_8$; Albite: $NaAlSi_3O_8$.

Table 2
Tested formulations and some corresponding properties of hardened samples

Code	Solids composition (wt.%)	*b*/*a* ratio	Kneading H_20 (%)	ρ_{geom} (g/cm^3)	*P* (%)	ρ_{satur} (g/cm^3)
L	100L	–	83	0.94	–	–
25L	75S+25L	1:3	26	1.48	27.0	1.57
33L	67S+33L	1:2	32	1.38	34.8	1.60
50L	50S+50L	1:1	46	1.19	50.2	1.57
Micro-L	75CS+25L	1:3	25.5	1.52	27.4	1.56
Cho-L	75CH+25L	1:3	25.5	1.47	29.4	1.56
20L20POZ	60S+20L+20BP	1:1:3	31	1.50	25.7	1.53
20L10POZ	70S+20L+10BP	2:1:7	21	1.57	23.5	1.56
10L20POZ	70S+10L+20BP	1:2:7	18	1.61	20.6	1.62
HL	100HL	–	40.5	1.46	28.2	1.56
25HL	75S+25HL	1:3	19.5	1.62	21.4	1.58
20L20HL	60S+20L+20HL	1:1:3	27.5	1.49	29.2	1.60
20L10HL	70S+20L+10HL	2:1:7	25	1.53	25.3	1.61
10L20HL	70S+10L+20HL	1:2:7	22	1.63	23.2	1.58
Micro-HL	75CS+25HL	1:3	21	1.66	24.6	1.54
Cho-HL	75CH+25HL	1:3	16.5	1.75	20.3	1.58
C	100C	–	28	2.08	10.0	1.74
25C	75S+25C	1:1:3	19	1.74	15.2	1.70
20L20C	60S+20L+20C	1:2	25	1.64	23.5	1.63
20L10C	70S+20L+10C	2:1:7	25	1.59	25.8	1.54
20L5C	75S+20L+5C	2:0.5:7.5	33.5	1.58	22.8	1.60
10L20C	70S+10L+20C	1:2:7	19	1.81	17.7	1.64
Micro-C	75CS+25C	1:3	13.5	1.84	16.0	1.60
Cho-C	75CH+25C	1:3	15	1.87	12.5	1.66
20G	80S+20G	1:4	15	1.61	11.1	1.98
25G	75S+25G	1:3	15	1.53	15.1	2.23
33G	67S+33G	1:2	17	1.56	14.9	1.92
50G	50S+50G	1:1	21	1.50	20.2	1.76
20G20L	60S+20G+20L	1:1:3	21	1.39	29.2	1.72
20G20HL	60S+20G+20HL	1:1:3	21	1.62	16.5	1.80
20G20C	60S+20G+20C	1:1:3	18	1.70	21.9	1.66

b/*a*=binder:aggregates ratio; ρ_{geom}=geometrical density; ρ_{satur}=apparent density (determined by saturation); *P*=porosity. S=sand; L=lime; C=cement; HL=hydraulic lime; BP=bricks powder; G=gypsum; CS=calcareous sand ("Micromar"); CH=coarser quartz sand ("Chorreio"). Standard deviations are below 10% of the mean value.

constituted only of binder (L-100% lime, HL-100% hydraulic lime or C-100% cement), and also gives the amount of kneading water used to reach a suitable workability.

After preparation, samples were placed in an acclimatised chamber during 90 days, keeping the temperature and the relative humidity constant (T=23±2 °C; H=50±5%). Some samples (those made of 100% binder) were placed in a carbonation chamber, to force the complete carbonation. The chamber operates at $P(CO_2)$=0.2 bar, T=25±1 °C; H=80±10%, and the carbonation degree was tested with phenolphthalein (the observation of a pink colour corresponds to the existence of portlandite).

2.2. Analyses

For all determinations an average of at least three sample measurements was used, in accordance to EN1015 [13]. The apparent density of cured mortars was evaluated by two different ways: (i) weight/geometric evaluation by using prismatic samples of well defined shape; (ii) saturation method, by weighting the sample in different conditions (dried, m_d,

immersed in water for 24 h, m_i, and immediately after immersion, m_h) and by applying the following equations for apparent density (ρ) and open porosity (P):

$$\rho = \frac{m_d}{m_i - m_h} \quad (1)$$

$$P = \frac{m_i - m_d}{m_i - m_h} \quad (2)$$

The first method is only applicable when well shaped samples are available, which is difficult to achieve with removed pieces of old mortars. The saturation method also allows the estimation of open porosity, by using Eq. (2) [13]. However, pure lime samples cannot be tested in this way, since they react and disintegrate in the presence of water.

The mechanical characterization of hardened mortars involves measurements of dynamic elastic modulus, and flexural and compression strengths, following standard methods (EN 1015). Elastic modulus determinations of gypsum-based samples were not performed, since the required large samples were too fragile and collapsed when pulled out of the mould. This difficulty also occurred with the 100% lime-based sample (L).

The main constituents of prepared samples were determined by XRD (Rigaku Geigerflex D/max Series, Cu-kα radiation, between 4° and 80° (2θ), with a scanning speed of 3°/min) and by differential and thermogravimetric thermal analyses (DTA/TGA, SETARAM-LabSys, heating rate of 5 °C/min, up to 1000 °C).

3. Results and discussion

3.1. Comparative characterization

Fig. 1 gives the porosity of hardened samples as function of aggregates relative amount. Lime-based mortars are clearly more porous than gypsum and cement-based materials, this being a consequence of the need for using higher amounts of kneading water to reach acceptable workability. This effect is particularly severe in the pure-lime formulation without aggregates. In all cases, porosity tends to diminish by increasing the relative amount of aggregates, again as a reflex of the use of lower amounts of water. For mortars prepared with the same binder and having a fixed relative amount of aggregates (e.g., 75 wt.%), the observed differences are related to the nature of the aggregates and, in particular, with its particle size distribution, but no relation is applicable that encompasses all types of binders. Anyway, the values do not vary too much between themselves. In lime mortars the lowest porosity is from the siliceous sand sample, while in hydraulic lime and in cement mortars "chorreio" aggregates give the lowest porosity, despite their bigger grain size.

Table 3 presents the relevant values of mechanical properties. It is easy to confirm the expected proportionality between compressive and flexure strength values, as shown in Fig. 2. At the same time, the dynamic elastic modulus follows a similar evolution. Mechanically weaker samples are those having higher

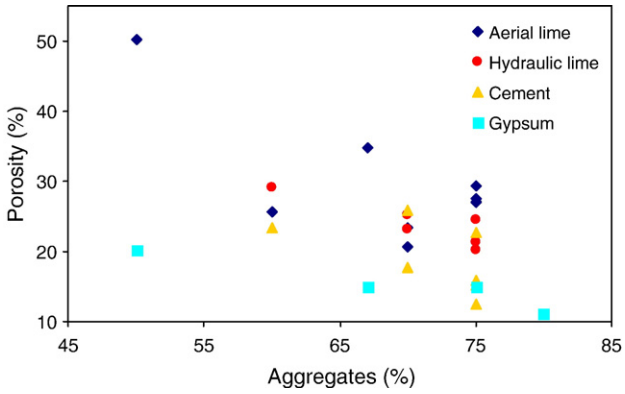

Fig. 1. Change of the porosity of mortars as a function of aggregates content and binder type. Pozzolan-containing (BP) lime mortars are considered as lime binders.

amount of voids that correspond to a decrease of the measured resonant frequency and apparent density, which have a direct influence (decreasing) over the elastic modulus. 100% HL sample presents a curious behaviour. Although it has a slightly higher porosity (~28%) it has developed the highest mechanical strength amongst all hydraulic lime samples. This result was double checked and can only be related to the development of a specific microstructure, due to the absence of sand. By comparing the mechanical resistance of mortars prepared from different binders, the following increasing sequence, as expected, is observed: gypsum < aerial lime < hydraulic lime < cement (Fig. 2). The performance of samples prepared with hydraulic lime is much closer to those based on aerial lime than to the cement-based ones, suggesting that the hydraulic lime used does not show a strong hydraulic character. However, higher mechanical resistances were always obtained when compared to aerial lime mortars. Tests at higher curing times (>90 days) can clarify this aspect, and will certainly show an enhancement of the hydraulic lime mortars mechanical properties. Pozzolan-containing samples also develop mechanical resistances similar to those based on aerial lime, suggesting that their pozzolanic activity is not very effective, at least for the tested period (90 days). This is due to the low reactivity of the used brick powder, probably due to their processing temperature. It is well established that the better pozzolanic ceramics powder are finely pulverized and fired at temperatures in the range of 600–900 °C [5,11].

As expected, combined mortars (made by the combination of two binders) have intermediate mechanical properties when compared with values of mortars prepared by each single binder. These values do not necessarily change linearly with the relative amount of each binder. For example, combined mortars containing aerial lime as the main binder plus small additions of hydraulic lime or cement, show only slight differences to pure aerial lime-based materials. So, the intention of improving the mechanical behaviour of aerial lime mortars by adding small amounts of hydraulic binders was not achieved in these formulations.

Samples made of single binders without aggregates show better mechanical resistance, except the one made of aerial lime. The presence of aggregates should improve the mechanical

Table 3
Mechanical properties of the samples

Code	R_c (MPa)	R_f (MPa)	ε (MPa)	Code	R_c (MPa)	R_f (MPa)	ε (MPa)
L	0.74	0.29	–	C	26.64	5.86	30,295
25L	1.56	0.53	4435	25C	19.04	3.21	17,190
33L	1.53	0.59	4714	20L20C	8.77	1.81	12,594
50L	1.23	0.46	2856	20L10C	2.79	0.86	8803
Micro-L	1.63	0.59	7202	20L5C	1.46	0.60	4870
Cho-L	0.59	0.40	5133	10L20C	11.31	2.95	18,408
20L20POZ	1.38	0.53	5086	Micro-C	15.94	4.53	16,731
20L10POZ	1.36	0.54	5621	Cho-C	18.91	4.03	21,576
10L20POZ	1.23	0.51	4321	20G	0.24	0.13	–
HL	7.01	0.98	8166	25G	0.48	0.15	–
25HL	2.79	0.87	6089	33G	0.52	0.21	–
20L20HL	2.19	0.57	6196	50G	0.52	0.25	–
20L10HL	1.52	0.42	4690	20G20L	1.39	0.38	5920
10L20HL	2.65	0.74	5781	20G20HL	2.45	0.80	8012
Micro-HL	1.85	0.58	7872	20G20C	5.98	2.09	12,643
Cho-HL	2.23	0.56	10,503				

(R_f=flexural strength; R_c=compression strength; ε=elastic modulus. Standard deviations are below 10% of the mean value).

performance, once optimised mixing conditions and a compact microstructure is achieved. In the actual conditions, this requirement seems not to be satisfied and pure cement and hydraulic lime mortars show greater homogeneity.

By comparing mortars prepared with different aggregates, it seems that quartz sand tends to improve the mechanical behaviour in comparison with the calcareous aggregate. However, the use of coarser particles ("chorreio") creates the most unfavourable situation, due to structural disruptions in the material.

3.2. Distinctive characterization

As previously stated, the properties discussed above may be used for comparison purposes, once the most appropriate formulation for a specific restoration work is defined. This definition requires the previous characterization of the old mortar by accurate means. For this, the prepared samples were characterized by XRD and DTA/TGA analyses.

Table 4 details the main crystalline phases detected by XRD. As expected, quartz is the most visible component, confirming the benefits of this technique in the aggregates identification. However, its typical high crystallinity might superimpose over minor peaks of less-crystalline phase, as those corresponding to the hydraulic components. Differences between mortars composed by distinct binders are also clear. Specific peaks of gypsum, aerial and hydraulic binders (hydraulic lime or cement) are well distinctive. Gypsum mortars are distinguished by calcium sulphate diffraction peaks (Fig. 3a). Aerial lime formulations are identified by calcite peaks and, portlandite might eventually be present if the carbonation process is not complete (Fig. 3b). This happened with samples not exposed inside the carbonation chamber due to their relatively short curing time. When calcareous aggregates are present calcite peaks are much more intense but the contribution of the binder is impossible to distinguish. However, quartz peaks are also observed, not as a trace but as a well crystallised phase.

Differences between mortars based on different hydraulic binders (lime and cement) are more difficult to detect, as can be concluded by analysing Fig. 4. Main peaks correspond to calcite, dicalcium silicate (belite), and tricalcium silicates (alite and hatrurite). These silicates are predictably in high amounts in Portland cement, but the processing conditions of the hydraulic lime used here also favoured their formation in reasonable

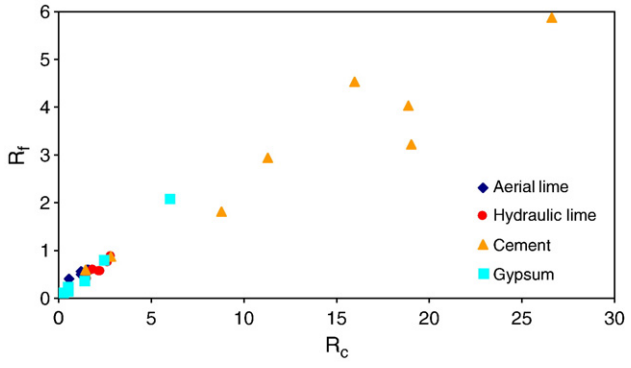

Fig. 2. Relationship between flexural (R_f) and compression (R_c) strength of some hardened (90 days) mortars in function of binder type. Hydraulic samples are clearly more resistant, in particular those containing cement.

Table 4
Phases identified by XRD on hardened samples

Sample code	Phases
L	Calcite, quartz
25L	Calcite, portlandite, quartz
33L	Calcite, portlandite, quartz
50L	Calcite, portlandite, quartz
Micro-L	Calcite, portlandite, dolomite, quartz
Cho-L	Calcite, portlandite, quartz
20L20POZ	Calcite, portlandite, quartz
20L10POZ	Calcite, portlandite, quartz
10L20POZ	Calcite, portlandite, quartz
HL	Calcite, quartz, ettringite, alite, microcline
25HL	Calcite, quartz, alite, ettringite
20L20HL	Calcite, portlandite, quartz, ettringite
20L10HL	Calcite, portlandite, quartz, ettringite
10L20HL	Calcite, portlandite, quartz, ettringite
Micro-HL	Calcite, portlandite, quartz
Cho-HL	Calcite, quartz, microcline, ettringite
C	Calcite, quartz, ettringite, alite, belite, gypsum, hatrurite
25C	Calcite, portlandite, quartz, belite, alite
20L20C	Calcite, portlandite, quartz, alite
20L10C	Calcite, portlandite, quartz
20L5C	Calcite, portlandite, quartz
10L20C	Calcite, portlandite, quartz, alite, ettringite
Micro-C	Calcite, portlandite, quartz, alite
Cho-C	Calcite, portlandite, quartz, alite, ettringite
20G	Gypsum, quartz
25G	Gypsum, quartz
33G	Gypsum, quartz
50G	Gypsum, quartz
20G20L	Gypsum, calcite, portlandite, quartz
20G20HL	Gypsum, calcite, portlandite, ettringite, quartz
20G20C	Gypsum, calcite, portlandite, ettringite, alite, quartz

Calcite: $CaCO_3$; Quartz: SiO_2; Portlandite: $Ca(OH)_2$; Dolomite: $CaMg(CO_3)_2$; Ettringite: $Ca_6Al_2(SO_4)_3(OH)_{12}{:}26H_2O$; Alite: Ca_3SiO_5; Belite: Ca_2SiO_4; Microcline: $KAlSi_3O_8$; Hatrurite: Ca_3SiO_5; Gypsum: $CaSO_4{:}2H_2O$.

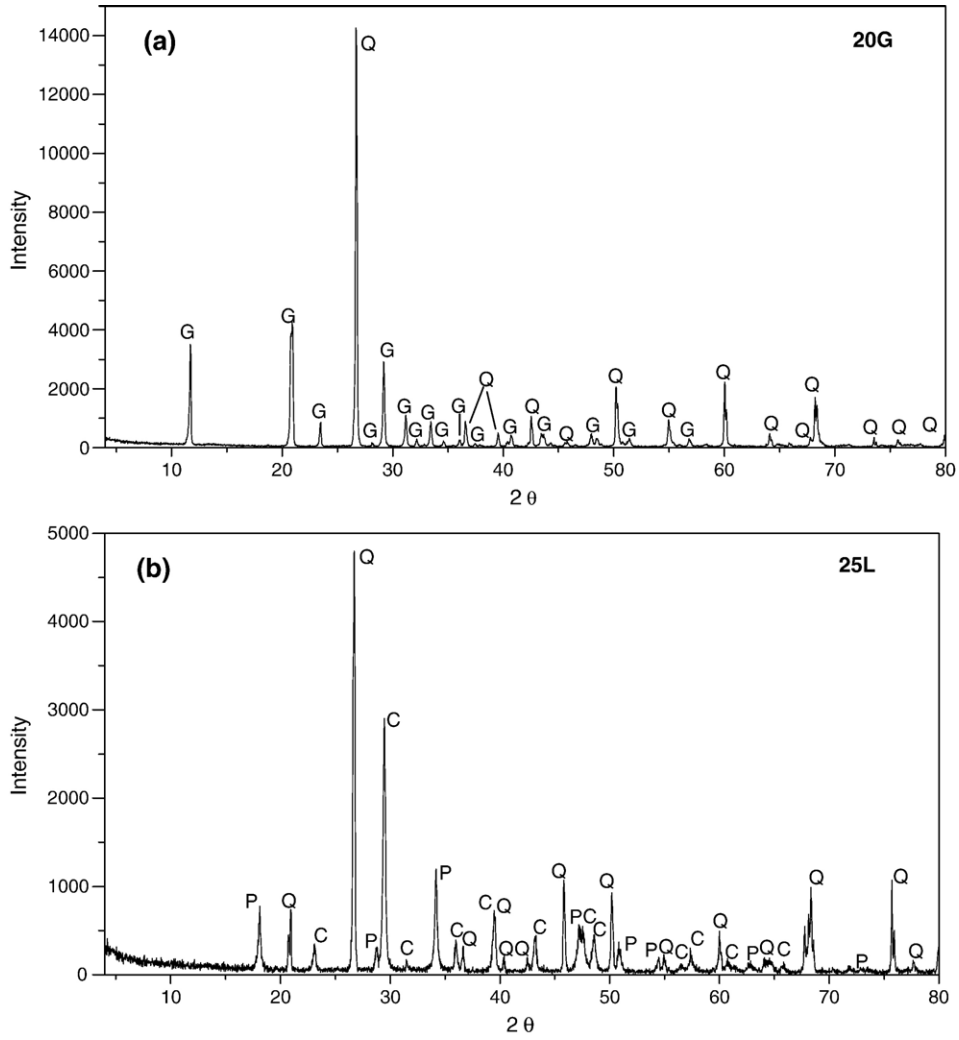

Fig. 3. XRD patterns of 20G (a) and 25L (b) samples, denoting the presence of gypsum (G), calcite (C), quartz (Q), and portlandite (P).

amounts. Less intense peaks of quartz, portlandite, ettringite, and feldspars are also visible, naming those potentially more useful to characterize the material.

The identification of phases in combined mortars is, as expected, more complex, but distinctive peaks are always possible to observe. The use of clay-based pozzolans (i.e. binders containing powdered bricks and terracotta) might also create extra difficulties, since micaceous phases, feldspars, wollastonite, melilite, pyroxenes are present. The complexity of the systems and lack of separation between patterns of several phases strongly restrict the potential of XRD as the main distinctive tool for the study of mortars. As suggested elsewhere [14], the previous removal of aggregates before the analysis helps in clarifying the binder nature.

DTA/TGA analyses complement the XRD results, and in some cases are even more useful in distinguishing gypsum, aerial lime and hydraulic-based mortars. Table 5 details all weight losses which occurred in tested mortars, when fired up to 1000 °C. The first loss, observed in all mortars, corresponds to the removal of hygroscopic water and occurs up to 120 °C. Differences between distinct groups, according to the binder nature, arise at higher temperatures, as it is illustrated in Fig. 5.

Gypsum-based mortars show a significant weight loss up to 200 °C. The evaluation of the amount of gypsum might be obtained taking into account that each molecule of $CaSO_4$ partially decomposes two water molecules at temperatures between 120–150 °C, forming the hemi-hydrate, $CaSO_4 \cdot 1/2H_2O$. In DTA this decomposition is noted by a doublet of endothermic peaks. Table 5 also shows the estimated quantification of gypsum amounts, confirming the usefulness of this approach, since estimated values are similar to those really used to prepare the mixtures (discounting the amount of kneading water). The small deviations are caused by the water decomposition from other components.

Another endothermic reaction, causing no weight changes, is observed at about 580 °C and corresponds to the $\alpha \rightarrow \beta$ quartz transformation. It occurs whenever quartz sand is used as aggregate (see Fig. 5b,d). The detection of an unexpected slight endothermic reaction above 700 °C (CO_2 decomposition), responsible for the observed weight loss (Fig. 5a), suggests the existence of lime and proves that the material is somewhat impure.

At this point it is important to state that quantification of components must be used with precaution, because mortars may

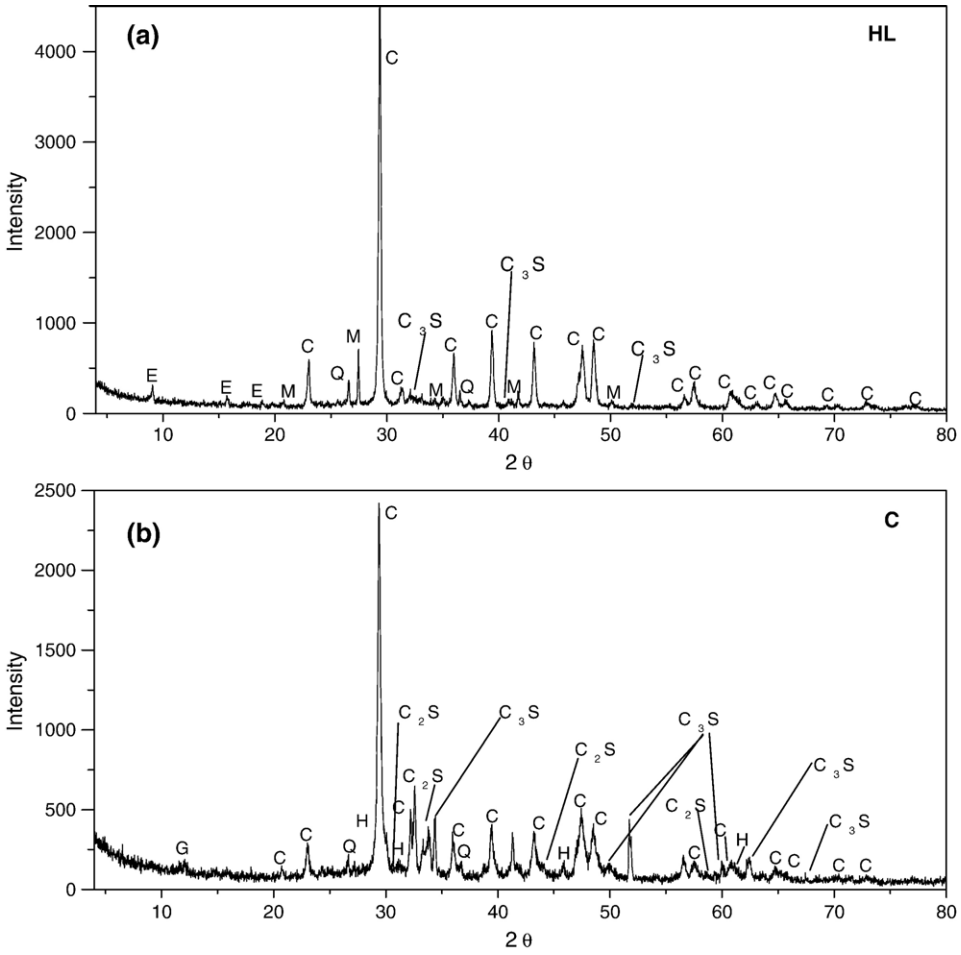

Fig. 4. XRD patterns of HL (a) and cement (b) pure mortars: calcite: C; quartz: Q; ettringite: E; microcline: M; alite: C_3S; belite: C_2S; hatrurite: H.

not have passed through the complete curing process at the time of analyses. This aspect is particularly relevant in mortars with long curing periods, like those based on aerial lime. However, identification of compounds is very reliable when using DTA/TGA and this semi-quantification can give a clear suggestion of the contribution of each single component.

DTA/TGA patterns of combined gypsum mortars show cumulative typical decomposition peaks of each component: the mentioned weight loss of $CaSO_4$ decomposition plus (i) the weight loss corresponding to calcium carbonate decomposition in the interval 750–850 °C (gypsum + aerial lime mortars), or (ii) weight losses at 200–600 °C, due to decomposition of hydraulic components (G + HL and G + C mixtures).

For quantification of calcium carbonate, the observed decomposition at 750–860 °C can be used, taking into account that each molecule of $CaCO_3$ frees one CO_2 molecule. However, two situations can be distinguished: (i) when decomposition is restricted to the 750–860 °C range, we may assume that recarbonated calcite is present, and weight loss is just caused by the lime binder (25L — Fig. 5b); (ii) when the reaction is extended to the 750–950 °C range, CO_2 decomposition is also attributed to the presence of calcareous aggregates. Since the typical particle size of aggregates is higher, decomposition tends to occur at higher temperature (see Micro-L in Fig. 5c) [7,14]. The use of a simple molar correspondence between $CaCO_3$ and $Ca(OH)_2$ allows us to estimate approximately the amount of hydrated lime or portlandite in the initial mixture, once discounting the kneading water. The endothermic peak and corresponding weight loss at 480 °C were not detected. It should be noticed that the direct estimation of hydraulic-type amount in the initial mixture is not possible using this technique, since several varieties of hydraulic components can be present and their correct molar fractions are not fixed. The sum of estimated amounts of portlandite and recarbonated calcite will correspond more or less to the total hydrated lime of the initial mixture. It is easy to verify that calculated and expected (from known formulations) values are close.

In all aerial lime mortars, portlandite peaks are also present (except in the pure lime one, L), as already seen by XRD. This means that lime was not completely carbonated after 90 days, confirming the low rate of this process. The amount of portlandite seems to be higher in the Micro-L sample, for reasons not completely clarified. As expected, this sample shows a strong weight loss due to $CaCO_3$ aggregates decomposition.

DTA/TGA analyses of hydraulic-based (lime or cement) mortars are more complex and quantification of components are less accurate. The weight loss at up to 200 °C is higher than in aerial lime mortars (see Fig. 5d) and several endothermic peaks

Table 5
Thermogravimetric results of the hardened samples

Sample	<120 °C (%)	120–200 °C (%)	200–600 °C (%)	~480 °C (%)	700–850 °C (%)	750–860 °C (%)	700–950 °C (%)	750–950 °C (%)	% $CaSO_4 \cdot 2H_2O$	% Ca $(OH)_2$	Hr
L	1.7	1.6	2.4	0	0	37.2	0	0	–	62.56	15.50
25L	0.5	0	0.4	0.7	0	10.7	0	0	–	20.85	26.75
33L	0.3	0	0.5	0.6	0	12.2	0	0	–	22.96	24.40
50L	0.5	0	0.9	0.7	0	17.6	0	0	–	32.44	19.56
Micro-L	0.5	0	2.8	2.8	0	0	0	34.5	–	–	–
Cho-L	0.4	0.1	2.4	2.2	0	6.1	0	0	–	19.29	2.54
20L20POZ	0.5	0.2	0.6	0.7	0	6.1	0	0	–	13.13	10.17
20L10POZ	0.3	0	1.1	1.0	0	6.2	0	0	–	14.62	5.64
10L20POZ	0.4	0.2	0.5	0.3	0	2.8	0	0	–	5.93	5.60
HL	2.0	1.6	3.6	0	18.8	0	0	0	10.19	31.55	5.22
25HL	0.6	0.4	2.8	0	0	5.0	0	0	2.55	8.40	1.78
20L20HL	0.9	0.4	0.8	0.5	12.2	0	0	0	2.55	22.54	15.00
20L10HL	1.0	0.2	2.0	2.3	5.8	0	0	0	1.27	18.59	2.90
10L20HL	0.8	0.3	1.3	0.8	7.0	0	0	0	1.91	15.05	5.38
Micro-HL	0.8	0.2	1.4	0.3	0	0	35.7	0	1.27	–	–
Cho-HL	0.6	0.6	1.4	0	0	5.0	0	0	3.82	8.40	3.57
C	2.8	1.9	5.3	0	7.6	0	0	0	12.10	12.80	2.42
25C	1.3	0.7	2.0	0.5	2.2	0	0	0	4.46	5.76	1.10
20L20C	1.7	1.0	3.0	2.2	7.0	0	0	0	6.37	20.80	2.33
20L10C	0.7	1.0	1.5	1.0	7.0	0	0	0	6.37	15.87	4.67
20L5C	0.4	0.3	0.8	0.6	0	8.0	0	0	1.91	15.90	10.00
10L20C	1.9	1.1	3.0	1.5	3.0	0	0	0	7.01	11.20	1.00
Micro-C	1.5	1.0	1.7	0.5	0	0	31.4	0	6.37	–	–
Cho-C	1.2	1.3	3.5	0.8	3.3	0	0	0	8.28	8.83	0.94
20G	0.3	3.4	0.2	0	0	0.3	0	0	21.47	0.49	–
25G	0.1	3.4	0.3	0	0	0.2	0	0	21.72	0.34	–
33G	0.1	5.7	0.3	0	0	0.3	0	0	36.44	0.50	–
50G	0.2	9.0	0.3	0	0	0.4	0	0	57.33	0.70	–
20G20L	0.5	3.4	1.0	0.8	0	9.1	0.	0	21.78	18.66	–
20G20HL	0.8	3.4	0.4	0	3.1	0	0	0	21.53	5.27	–
20G20C	1.6	3.7	1.1	0.4	1.6	0	0	0	23.57	4.26	–

For the samples without calcareous aggregates the total percentage of hydrated lime was calculated, as well as the hydraulicity ratio (except in gypsum based mortars), which inversely reflects the hydraulic character of a mortar. The percentage of initial gypsum was also calculated.

are visible, caused by water decomposition of multiple hydraulic components. By refining the analysis, it is possible to quantify the amount of gypsum normally added to these mortars to act as a retarding agent for setting. In general, the weight loss observed in the region 200–600 °C is also higher, while calcium carbonate decomposition is weaker.

Moropoulou et al [7,15–18] defined a hydraulicity ratio (Hr) as the quotient between weight losses attributed to CO_2 (above 700 °C) and to water decomposition occurring in the intermediate temperature region (200–600 °C). This parameter inversely states the hydraulic character of a mortar. Hr values higher than 10 are typical for aerial lime mortars, while hydraulic mortars show values below that limit. Another subdivision might be assumed: (i) Hr values between 4 and 9 correspond to a weak hydraulic character; (ii) moderately hydraulic mortars (e.g., mortars containing clay-brick fragments) show values between 3 and 6; (iii) Hr inferior to 3 corresponds to strong hydraulic character (natural pozzolans or cement-based materials). This classification is naturally not valid when calcareous aggregates are present, since they also contribute to CO_2 decomposition. Again, great precaution must be used with this parameter, due to reasons already mentioned related with the quantification of compounds. Anyway, Table 5 lists calculated Hr values for the formulations used, permitting a relative estimation of the hydraulic level of the studied mortars. Note that this parameter will be slightly modified as hydraulic mortars develop through their curing processes.

In general, clear differences are noted between aerial lime and hydraulic-based samples. Mortars prepared with cement show the lowest Hr values, and lime mortars have values higher than 10. Even so, some misleading results are observed: 20L20HL shows a value of 15, despite the relatively high concentration of hydraulic lime; by contrast, Cho-L shows an extremely low value (2.54). Pozzolan-containing samples (20L10POZ and 10L20POZ) have hydraulicity ratios near 5, despite the apparent low hydraulic level and poor mechanical performance, as previously discussed. These discrepancies in Hr point out for that need of precaution in its calculation, when used to predict the performance or nature of mortars.

Another aspect that might help to distinguish between aerial (typical) and hydraulic lime or cement-based mortars is the existence of an inflection in the endothermic peak caused by calcite decomposition in DTA curves. Cement, hydraulic lime and hybrid (aerial lime+hydraulic compounds) mortars show this inflection, as exemplified in Figs. 5(d) and 6. The exception is the 20L5C material because of the relatively small amount of

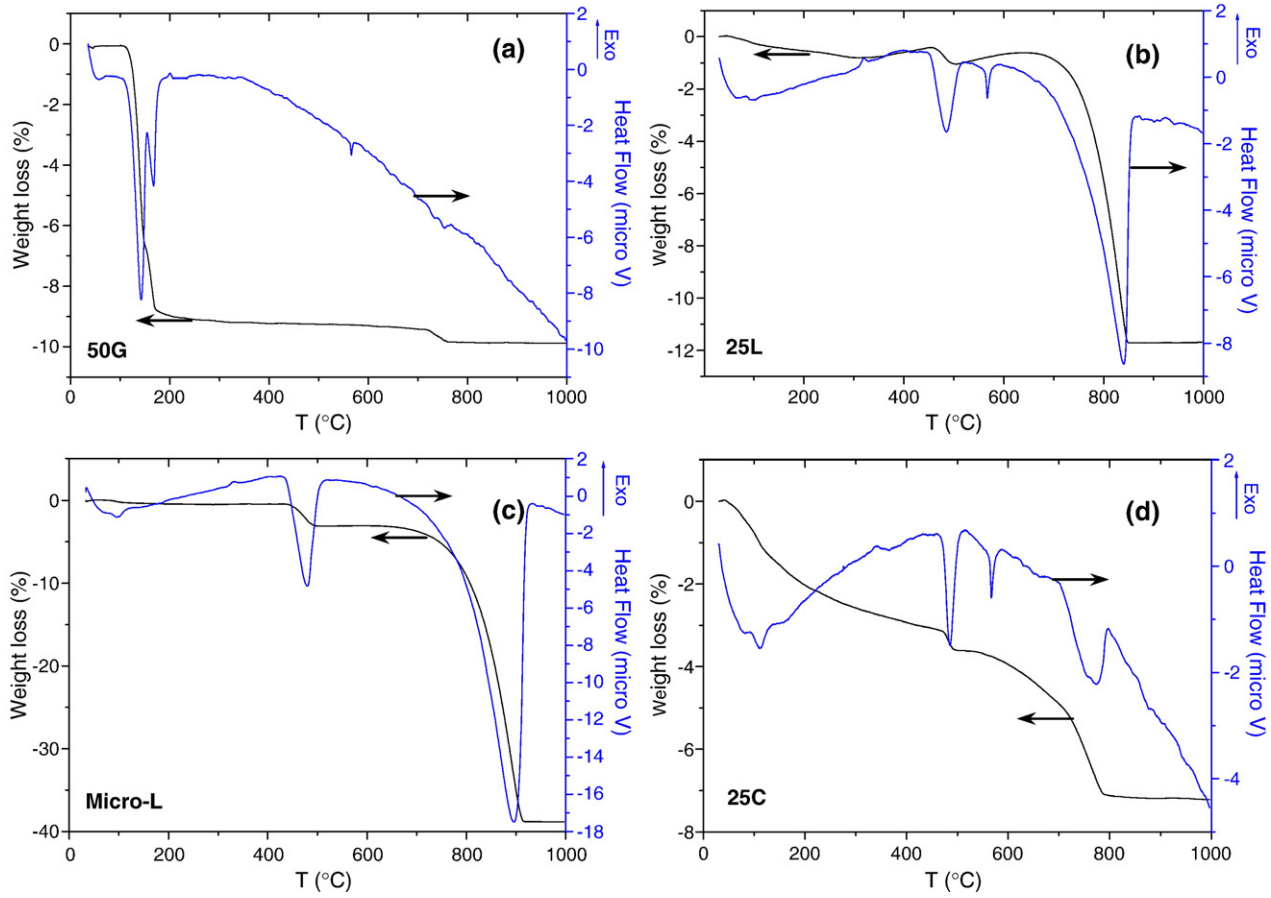

Fig. 5. DTA/TGA curves of representative mortars prepared from different binders: (a) 50G, (b) 25L, (c) Micro-L, and (d) 25C.

cement. Its hydraulicity ratio is about 10 and the mechanical resistance is very low, in the same order of magnitude as those made of aerial lime. The presence of dolomite could explain this doublet, but it was not identified by XRD in most hydraulic mortars. On the other hand, dolomite was identified in Micro-L sample (vestigial impurity), but no inflection is visible in DTA analysis. So it might be related with the existence of two types of lime, requiring slightly distinct energy levels to decompose. By TGA, no discontinuity is observed in the weight loss profile. Future use of DSC analysis might help to better refine this hypothesis.

At the moment it is relatively easy to correlate the chemical composition with physical and mechanical properties of most common mortars. At the same time, it is possible to emphasize the most significant aspects reached by each technique in the characterization of mortars. Gathering this information is important to the creation of a knowledge matrix of all tested formulations.

This matrix will be particularly useful to accelerate the rehabilitation process, searching for new formulations that are compatible from the chemical, physical and mechanical point of view with the old material. In other words, determining some characteristics of old mortars new formulation can be selected from the matrix that shows closer performance. Obviously, this matrix must be permanently under development and enrichment, by adding new studied formulations.

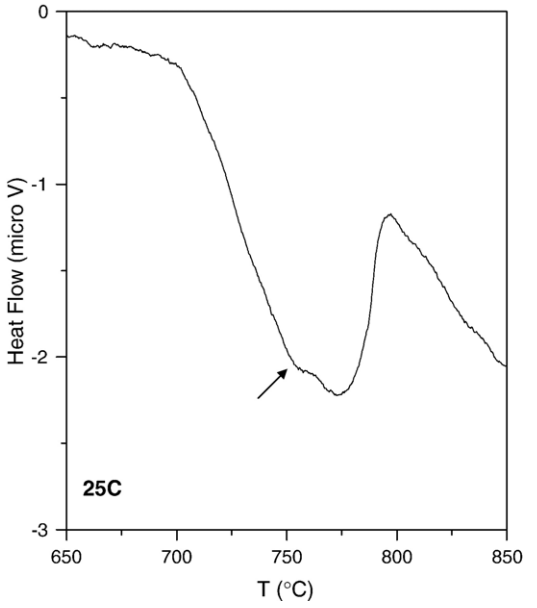

Fig. 6. Amplified view of the DTA/TGA of the 25C sample in the region of CO_2 decomposition.

4. Conclusions

The combined use of several techniques allows mortars to be distinguished and grouped according to type of binder and aggregate. The characterization methodology proposed here involved discriminative or distinctive and comparative determinations, and it was chosen with attention to the necessity of using quick and inexpensive analyses associated with a high degree of accuracy in common buildings rehabilitation practices.

Distinctive analyses attempt to define which are the main components and their relative proportions in the mortar. XRD and specially DTA/TGA analyses proved to be very useful for this purpose. Decomposition of components at specific temperature intervals and the hydraulicity ratio can give important hints on the mortars character.

The comparative characterization involves determination of performance indicators, such as physical (porosity, permeability, etc) and mechanical properties. This procedure attempts to assure the required compatibility between old and repaired mortars in each specific rehabilitation procedure.

By preparing and characterizing known selected formulations, this work attempted to build a matrix that can be used for the identification of old mortars and that also facilitates the selection of suitable and compatible repair ones.

Acknowledgment

Financial support by Materials Network for the Atlantic Area Project (Interreg IIIB- MNAA) is greatly appreciated (Sofia Marques).

References

[1] ICOMOS, 1964, http://www.icomos.org/docs/venice_charter.html.
[2] D. Carrington, P. Swallow, Limes and lime mortars — part two, Journal of Architectural Conservation 1 (1996) 7–22.
[3] Marques, Sofia MF; Estudo de argamassas de reabilitação de edifícios antigos, MSc Thesis, University of Aveiro, Portugal, 2005.
[4] C.A. Anagnostopoulos, A.C. Anagnostopoulos, Polymer-cement mortars for repairing ancient masonries mechanical properties, Construction and Building Materials 16 (2002) 379–384.
[5] John Warren, Conservation of Brick, Chap. 12 — Mortars, Renderings and Plasters, Butterworth Heinemann, England, 1999.
[6] M.R. Smith, L. Collis (Eds.), Aggregates. Sand, Gravel and Crushed Rock Aggregates for Construction Purposes, Geologycal Society, England, 1993.
[7] A. Moropoulou, A. Bakolas, K. Bisbikou, Characterization of ancient, byzantine and later historic mortars by thermal and X-ray diffraction techniques, Thermochimica Acta 269/270 (1995) 779–795.
[8] L. Paama, I. Pitkänen, H. Rönkkömäki, P. Perämäki, Thermal and infrared spectroscopic characterization of historical mortars, Thermochimica Acta 320 (1998) 127–133.
[9] M. Franzini, L. Leoni, M. Lezzerini, A procedure for determining the chemical composition of binder and aggregate in ancient mortars: its application to mortars from some medieval buildings in Pisa, Journal of Cultural Heritage 1 (2000) 365–373.
[10] P. Maravelaki-Kalaitzaki, A. Bakolas, A. Moropoulou, Physico–chemical study of Cretan ancient mortars, Cement and Concrete Research 33 (2003) 651–663.
[11] G. Baronio, L. Binda, Study of the pozzolanicity of some bricks and clays, Construction and Building Materials 11 (1997) 41–46.
[12] European Norm EN 998, Specification for Mortar for Masonry, Parts 1–2, 2003.
[13] European Norm EN 1015, Methods of Test for Mortar for Masonry, Parts 1–19, 1998–2002.
[14] A. Santos Silva, New approach in old mortars characterization, Proc. 3rd ENCORE, Lisbon, ed. LNEC, 2003, pp. 917–926.
[15] A. Moropoulou, A. Bakolas, S. Anagnostopoulou, Composite materials in ancient structures, Cement and Concrete Composites 27 (2005) 295–300.
[16] A. Moropoulou, A. Bakolas, K. Bisbikou, Investigation of the technology of historic mortars, Journal of Cultural Heritage 1 (2000) 45–58.
[17] A. Bakolas, G. Biscontin, A. Moropoulou, E. Zendri, Characterization of structural Byzantine mortars by thermogravimetric analysis, Thermochimica Acta 321 (1998) 151–160.
[18] G. Biscontin, M. Pellizon Birelli, E. Zendri, Characterization of binders employed in the manufacture of Venetian historical mortars, Journal of Cultural Heritage 3 (2002) 31–37.